Journal of the Serbian Chemical Society
JSCS-info@shd.org.rs • www.shd.org.rs/JSCS
J. Serb. Chem. Soc. 86 (5) 495–505 (2021)
JSCS–5437
Original scientific paper

Electrochemical oxidation of 2,4,6-trichlorophenol on iron-doped nanozirconia ceramic

NADICA D. ABAZOVIĆ[1], TATJANA D. SAVIĆ[1], TATJANA B. NOVAKOVIĆ[2], MIRJANA I. ČOMOR[1#] and ZORICA D. MOJOVIĆ[2*]

[1]*Vinča Institute of Nuclear Sciences – National Institute of the Republic of Serbia, University of Belgrade, P.O. Box 522, 11000 Belgrade, Serbia and* [2]*University of Belgrade – Institute of Chemistry, Technology and Metallurgy – National Institute of the Republic of Serbia, Njegoševa 12, 11000 Belgrade, Serbia*

(Received 4 August, revised 13 November, accepted 30 November 2020)

Abstract: Solvothermaly synthesized zirconium oxide nanopowders, pure and doped with various amounts of iron ions (1–20 %), were used as modifiers of glassy carbon electrodes. The modified electrodes were tested in the reaction of electrochemical oxidation of 2,4,6-trichlorophenol (TCP) in order to investigate the influence of doping on electrochemical performance of zirconia matrix. The techniques of cyclic voltammetry and electrochemical impedance spectroscopy were employed. Cyclic voltammetry showed that electrooxidation of TCP proceeded through the oxidation of hydroxyl group. Possible pathway included the formation of quinones and the formation of polyphenol film on the electrode surface, leading to the electrode fouling. Iron doping enhanced the activity of zirconia matrix towards TCP electrooxidation. Electrochemical impedance spectroscopy showed the importance of iron content in zirconia matrix for the preferable pathway of TCP electrooxidation. The quinone formation pathway was favoured by low iron doped zirconia (doped with 1% of iron), while polyphenol film formation on the electrode surface was more pronounced at samples with higher iron ion content (for doping with 10 and 20 % of iron). The sample with 5 % of added iron ions, showed intermediate behaviour, where the formed polyphenol film showed slight degradation.

Keywords: ZrO_2; modified electrode; phenols.

INTRODUCTION

The extensive pollution is a worldwide problem today. Various pollutants, organic and inorganic, are being emitted and accumulated in different parts of the environment. Water pollution by phenol and its derivatives is recognized as a particular problem and addressed in a great number of articles. Europian Union,

* Corresponding author. E-mail: zoricam@nanosys.ihtm.bg.ac.rs
# Serbian Chemical Society member.
https://doi.org/10.2298/JSC200804078A

World Health Organization and American Environment Protection Agency have adopted the list of phenolic compounds that are considered as major pollutants. Among these pollutants chlorophenols are considered to be the most toxic and cancerous. Various methods have been investigated in order to detect[1–4] and remove[5–8] chlorophenols from water.

Electrochemical techniques attracted lot of attention because they are swift, efficient and low-cost. Additionally, the potential control enables easy and fine tuning of reaction. Various electrodes have been used to detect[9,10] and degrade[11–13] phenol compounds. Ureta-Zañartu *et. al.* investigated the mechanism of electrooxidation of phenol and phenol derivatives[14–20] on different electrodes. They concluded that there can be two possible pathways for the chlorophenol electrooxidation that proceeded to the formation of quinones or polymerization. The concentration of chlorophenol, the number of chlorine atoms and their position influences a preferable pathway, as well as a type of electrode.

Zirconia is eco-friendly ceramic material interesting as catalyst,[21] catalyst support[22] or photocatalyst,[23] being the only metal oxide material which, depending on crystal phase, can possess both Brønsted and Lewis acid and basic surface sites, and strong oxidizing and reducing ability[24]. However, since it is a wide band gap material ($E_g \approx 5.0$ eV) with the absorption edge placed deep in UV region of solar spectrum, its extensive application as photocatalyst is somewhat hindered. Various approaches have been developed to shift its spectral response towards the visible part of the spectrum, and among these, the doping of zirconia matrix with transition metal ions is a common strategy. In our previous study,[25] we have presented the synthesis and the detailed characterization of the series of iron doped zirconia samples (from 1 up to 20 wt.% of Fe^{3+}). Lower iron concentrations stabilized tetragonal crystal phase of zirconia, while for the highest dopant concentration (20 wt.%), beside tetragonal zirconia, hematite is also formed. The synthesized samples were probed in the photocatalytic degradation of 2,4,6-trichlorophenol (TCP) under simulated solar light. It was shown that photocatalytic activity greatly depends on the amount of added iron and on the formation of a great number of intraband defect sites (oxygen vacancies, Fe^{3+}/Fe^{2+} and Fe^{3+}/Fe^{4+} levels). Comparing two extremes: doped (1 wt.% Fe^{3+}) and composite (hematite/tetragonal zirconia) sample (20 wt.% Fe^{3+}), it turned out that the sample with lower iron content expressed higher efficiency toward TCP degradation. As far as we are aware, the electrochemical properties and the possible use of iron doped zirconia as the electrode material is studied previously only by Doménech-Carbó and Alarcón.[26,27]

In the present study, the effect of iron doping of zirconia on electrochemical oxidation of TCP was investigated. The iron-doped zirconia was used as modifier of glassy carbon electrodes. The electrochemical behaviour and electrocatalytic

properties were studied by cyclic voltammetry and electrochemical impedance spectroscopy.

EXPERIMENTAL

The solvothermal synthesis of pure and iron doped zirconium oxide nanopowders is presented elsewere.[25] Shortly, the appropriate amounts of iron (III) acetylacetonate and zirconium propoxide (70%) were mixed in acidic medium in a Teflon vessel and stirred vigorously in ice bath. After 15 min of stirring, the dispersion was autoclaved 24 h at 150 °C. The obtained powders were washed, dried weight and annealed at 600 °C for 3 h. The samples were denoted according to stoichiometric quantities of Fe ions, as ZrO_2, 1-ZrO_2, 5-ZrO_2, 10-ZrO_2 and 20-ZrO_2 (for 0, 1, 5, 10 and 20 wt.% of iron ions, respectively). The results of the detailed characterization are presented elsewhere.[25]

In order to use the investigated materials as electrode materials, 5 mg of each of the samples were homogeneously dispersed in 125 μl of the original 5 % Nafion solution, using an ultrasonic bath for 30 min. The droplets (10 μl) of these suspensions were placed on the surface of a glassy carbon electrode (GCE) (area = 0.0706 cm^2) and left to dry at 90 °C during 3h. After the solvent evaporation, the sample was uniformly distributed on the GCE in the form of a thin layer. For the electrochemical investigations in a three-electrode glass cell, the modified GCE, was used as working electrode. The reference electrode was Ag/AgCl in 3 M KCl, while a platinum foil served as a counter electrode. The electrochemical behaviour of samples was investigated in 0.1 M H_2SO_4 supporting electrolyte. TCP oxidation was investigated for the concentration of TCP of 1 mM in 0.1 M H_2SO_4. The electrochemical measurements were performed using Autolab electrochemical workstation (Autolab PGSTAT302N, Metrohm-Autolab BV, Netherlands). Cyclic voltammetry was performed at scan rate of 50 mV s^{-1}. Impedance measurements were carried out at constant potential using a 5 mV rms sinusoidal modulation in the 10 kHz–10 mHz frequency range.

RESULTS AND DISCUSSION

Electrochemical behavior of zirconia modified GCE in 0.1 M H_2SO_4

Cyclic voltammograms of ZrO_2 and iron-doped ZrO_2 modified GCE were recorded in 0.1 M H_2SO_4 at the scan rate of 50 mV s^{-1} (Fig. 1).

The potential range was chosen to encompass hydrogen and oxygen evolution at the potential range limits. Beside current the rise at the limits of the potential range due to hydrogen and oxygen evolution reaction, there is only one pair of redox peak at the potential of 0.55 V *vs.* Ag/AgCl. This pair of peaks can be ascribed to the Fe^{2+}/Fe^{3+} oxidation/reduction process. The intensity of the peak current rised with the increase of the Fe content in samples. The electrochemistry of iron oxides and iron doped zircon and zirconia was investigated by Doménech-Carbó *et al.*[26–28] The electrochemistry of solid materials on the electrode surface occurs at the three-phase boundary: solid sample, solid substrate electrode and electrolyte. Several processes can occur depending on the conductivity and solubility of the solid material: the oxidative dissolution of metals and alloys, the reductive dissolution of oxides and oxide hydrates and the reductive conversion of oxides and salts to metal deposits and dissolved anions. In the

media where protons are abundant, such as acid solution, the proton-promoted reductive dissolution of iron-species takes precedence:[26–28]

$$1/2Fe_2O_3 + 3H^+ + ne^- = (1–n)Fe^{3+} + nFe^{2+} + 3/2H_2O \quad (1)$$

$$FeO(OH) + 3H^+ + ne^- = (1–n)Fe^{3+} + nFe^{2+} + 2H_2O \quad (2)$$

The n value in above equations takes value 1 under condition that the medium is non-complexing, the proton-promoted dissolution is small and all dissolved iron is in Fe^{2+} form.

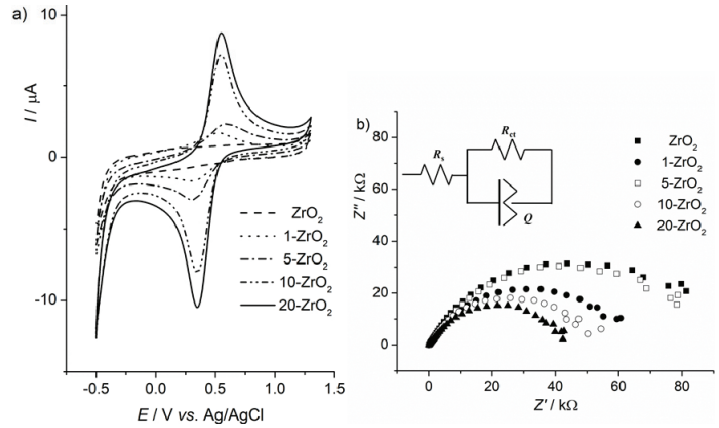

Fig 1. a) Cyclic voltammograms of ZrO_2 and iron-doped ZrO_2 in 0.1 M H_2SO_4, scan rate 50 mV s^{-1}; b) Nyquist plot for ZrO_2 and iron-doped ZrO_2 samples in 0.1 M H_2SO_4. Inset: equivalent electric circuit model used to fit experimental data.

According to the results of characterization[25] Fe ions were incorporated into the ZrO_2 matrix, in both crystalline phases and on the surface and in the bulk of nanoparticles. Also, in the sample with highest Fe^{3+} concentration, hematite can be detected. Slight decrease of current was noticed with the increase of cycling number that probably indicates the dissolution of iron species.

Further characterization of the samples was performed by the electrochemical impedance spectroscopy. For a modified electrode, the Nyquist plot recorded at 0.5 V showed a characteristic semi-circle pattern. The obtained EIS data (Fig. 1b) were used to fit an equivalent electrical circuit model (Fig. 1b, inset). In this circuit model R_s represents the solution resistance, while R_{ct} and constant phase element (CPE) are the charge transfer resistance and the non-ideal capacitor, respectively. The values of R_s and R_{ct} were obtained as the intercept of the recorded curve with x-axis at high frequencies and low frequencies, respectively. CPE usually represents the double layer capacitance and can be described by following equation:

$$Z = 1/(Y_0(j\omega)^{\alpha}) \quad (3)$$

where Y_0 is CPE admittance, j is the imaginary unit, ω is the angular frequency and α is CPE exponent which is associated with the system inhomogeneity. The capacitance element CPE would be pure capacitance when $\alpha = 1$ while it would be pure resistance when $\alpha = 0$. For the values $0.5 < \alpha < 1$ CPE is the non-ideal capacitor, which is influenced by surface heterogeneity. The values of circuit elements obtained by fitting were presented in Table I.

TABLE I. The electrochemical parameters extracted from the EIS data recorded in 0.1 M H_2SO_4 (R_s – the solution resistance; R_{ct} – the charge transfer resistance; Y_0 – CPE admittance, n – CPE exponent)

Sample	R_s / Ω	R_{ct} / kΩ	Y_0 / μS s^n	α
ZrO_2	60.9	105.3	6.26	0.73
1-ZrO_2	52.8	79.6	7.81	0.66
5-ZrO_2	54.6	104.1	5.99	0.69
10-ZrO_2	58.0	54.4	5.55	0.76
20-ZrO_2	51.5	45.9	5.68	0.74

The solution resistance, R_s, is almost constant (51–61 Ω) for all investigated samples. The charge transfer resistance, R_{ct}, had the highest value for ZrO_2, and this value decreased with the increase of Fe content in the samples. The only exception was sample 5-ZrO_2 that had charge transfer resistance almost equal to the starting material. The possible explanation might be the partial formation of zirconium ferrite, leaving much fewer Fe^{3+} for doping of zirconia matrix.[25] The admittance is proportional to the surface area involved in the electrochemical reaction.[29] There was no great variation in the values of admittance, although the highest admittance value was obtained for 1-ZrO_2 sample.

Electrochemical behavior of zirconia modified GCE in 0.1 M H_2SO_4 in the presence of TCP

Fresh GCE modified with zirconia was placed in the 0.1 M H_2SO_4 solution containing 1 mM TCP. The cycling of all electrodes measured in the potential range of –0.5 to 1.3 V, produced the family of voltammogram curves. The representative family of curves obtained for 5-ZrO_2 modified GCE is presented in Fig. 2a.

The irreversible anodic peak at 0.93 V, designated as a, corresponded to the oxidation of hydroxyl group at TCP. The peak current slightly decreased with cycling, which is considered as electrode fouling, due to the formation of polyphenol film.[30] The reversible pair of peaks (a2/c2) at lower potential was ascribed to the formation of quinones, and the anodic peak currents increased with cycling. The cyclic voltammograms of all investigated samples in 0.1 M H_2SO_4 containing 1 mM TCP had similar shape (Fig. 2b). The comparison of investigated modified electrodes was performed by the voltametric parameters obtained from cyclic voltammograms presented in Fig. 2b (Table II).

The onset potential is the potential at the foot of peak wave when the current starts to increase, *i.e.*, the potential that is necessary to reach for faradic current to

rise above capacitive current. As the indicator of electrode activity, the onset potential is particularly useful when the process that is investigated leads to the electrode fouling. The decreased values of onset potential were obtained for 1-ZrO_2 and 5-ZrO_2 samples, indicating higher electrode activity in comparison to undoped ZrO_2, 10- and 20-ZrO_2.

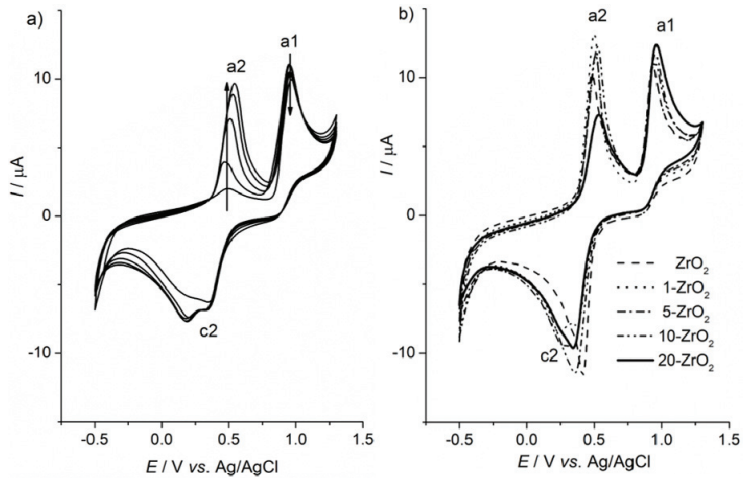

Fig 2. a) Successive cyclic voltammograms recorded on 5-ZrO_2. The arrows indicate the direction of peak current change with cycling; b) 5th cyclic voltammograms recorded on ZrO_2 and iron-doped ZrO_2 in 1 mM TCP + 0.1 M H_2SO_4, scan rate 50 mV s^{-1}.

TABLE II. The parameters obtained from cyclic voltammograms presented in Figure 2b: E_{a1} – peak potential of peak a1, E_o – onset potential for peak a1, Q – peak charge of designated peak

Sample	E_{a1} / V	E_o / V	Q_{a1} / μC	Q_{a2} / μC	Q_{c2} / μC	Q_{a2}/Q_{c2}	Q_{a2}/Q_{a1}
ZrO_2	0.93	0.82	0.73	0.98	1.01	0.97	1.34
1-ZrO_2	0.93	0.80	0.81	1.25	1.20	1.04	1.54
5-ZrO_2	0.94	0.81	0.90	1.19	1.21	0.98	1.32
10-ZrO_2	0.95	0.83	1.01	1.23	1.38	0.89	1.22
20-ZrO_2	0.96	0.82	1.08	0.71	1.11	0.64	0.66

The peak charge of peak a1 rises with the increase of the iron ion content in the zirconia sample on the GCE, indicating that the iron (iron oxide) enhanced the electrocatalytic activity of ZrO_2 for the oxidation of hydroxyl group of TCP. The highest current of TCP electrooxidation was obtained for 20-ZrO_2 electrode.

The oxidation of phenol and phenol derivatives usually produce one or two pair of reversible peaks due to formation of orto- or/and para-hydroquinone. In order to form quinones from TCP it is necessary to eliminate at least one of the chlorine atoms. The chlorine atom in para- position is the probable candidate due to less steric hindrance.[31] For samples with 1-ZrO_2 and 5-ZrO_2 the separation of

cathodic peak c2 was observed (Fig. 2a and b), which probably originated from the slight potential difference of iron reduction and hydroquinone formation. With the increase of the iron ions content, the potential difference between these two processes could not be observed any more. This finding implies the difference in iron ions properties/surroundings in the resulting samples formed at various iron ions content. These findings are in the accordance with our previous work,[25] where it was shown that samples with 10 and 20 % of iron ions have formed hematite phase, detected using XRD technique. 10-ZrO_2 and 20-ZrO_2 are actually composites of hematite and Fe-doped zirconia, i.e. iron ions exist as iron oxide and as dopant in zirconia matrix, while in the zirconia samples with lower iron ions content (1 and 5 %) iron ions exist only as dopants.

The ratio of the anodic to the cathodic charge of the hydroquinone/quinone process, (Q_{a2}/Q_{c2}), yields the reversibility of the hydro- quinone/quinone couple (Table II). The reversibility was almost equal for the undoped and the zirconia doped up to 5 % of Fe ions. The further increase of the iron ions content led to the decrease of the reversibility. The ratio Q_{a2}/Q_{a1} could be used to estimate the fraction of TCP oxidized to quinone[15]. These values were above unity except for 20-ZrO_2, and the highest value was obtained for 1-ZrO_2. This finding might indicate that the electrooxidation of TCP on samples with the high content of iron in zirconia matrix favours polyphenol film formation pathway. Bearing in mind that the oxido-reduction of iron ions zirconia matrix on the GCE occurs at similar potential as the formation of quinone, these features has to be taken with caution. Additionally, the cathodic peak currents did not show increase with the number of cycles, indicating a possible overlap of mentioned processes.

Further investigation of the electrochemical behaviour of TCP on zirconia samples was performed by the electrochemical impedance spectroscopy recorded at several potentials around the potential of oxidation of the hydroxide group of TCP: 0.80 (before peak potential), 0.93 (peak potential) and 1.10 V (after peak potential). The obtained Nyquist plots are presented in Fig. 3a–c.

The Nyquist plot recorded at peak potential consist of semicircle and straight line indicating the diffusion controlled Faradic process. The plot recorded at the potential 0.80 V shows characteristic semicircle obtained, indicating a charge transfer process, while the shape of plot recorded at 1.10 V showed the high resistance toward charge transfer process. The impedance data obtained at different potentials have been adjusted to the equivalent circuits presented in the inserted picture each Fig. 3a–c and the results are presented in Table III.

The equivalent circuit used for the plot recorded at peak potential contained two CPE corresponding to diffusion process (Q_1) and double layer capacitance (Q_2).

The charge transfer resistance at peak potential decreased with the increase of iron ions content present in samples, while the reverse trend was noticed for

potential of 1.10 V, probably due to fouling of the electrode surface by the polyphenol film.[15] Plot of the logarithm of the impedance, as a function of the potential at constant frequencies for ZrO_2, is presented in Fig. 3d. The plots obtained for other samples were similar and are not presented for the sake of clarity. The comparison of samples is presented in Fig. 3e as the plot of the logarithm of the impedance as a function of the potential at high frequency (10^4 Hz), *i.e.*, the resistance designated as R_s. The increase of impedance with potential indicates fouling of the electrode.[16] The impedance obtained for 1-ZrO_2 is higher than the impedance obtained for undoped ZrO_2, but the value remained constant with the increase of potential evidencing the absence of fouling. A slight decrease of impedance at potential of 1.10 V obtained for 5-ZrO_2 indicated some degradation of the formed polymer film. The samples with high content of iron (10 and 20 %) showed that fouling of the electrode is most likely to occur on these electrodes.

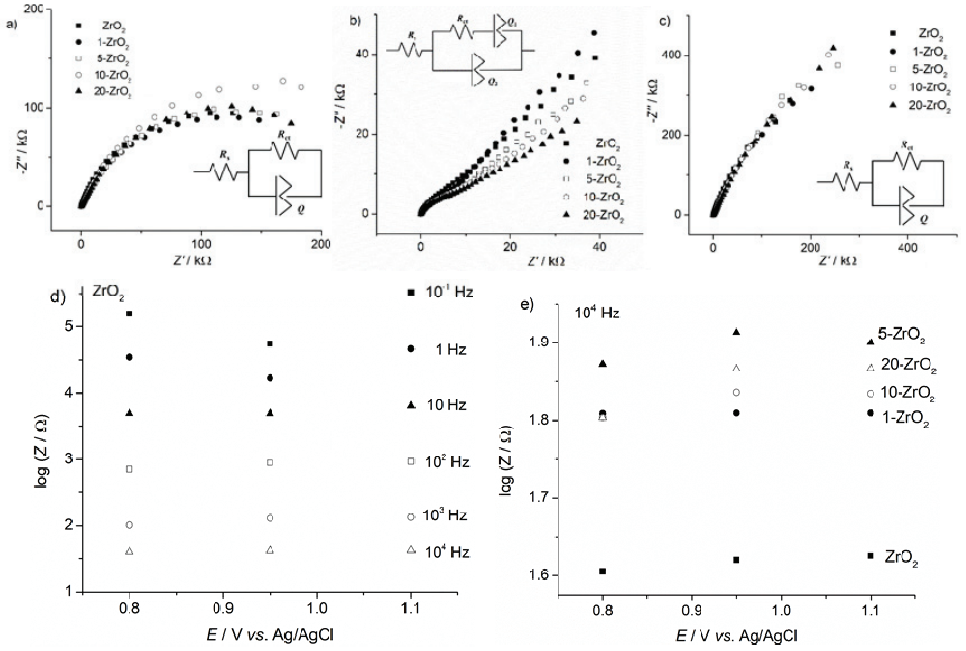

Fig 3. Nyquist plot for ZrO_2 and iron-doped ZrO_2 samples in 1 mM TCP + 0.1 M H_2SO_4 recorded at a) 0.80, b) 0.93 and c) 1.10 V (inset: equivalent electric circuit model used to fit experimental data.); d) plots of log|*Z*| *vs.* applied potential at the designated constant frequencies of a ZrO_2 electrode in 1 mM TCP + 0.1 M H_2SO_4; e) plots of log|*Z*| *vs.* applied potential at the frequency of 10^4 Hz for ZrO_2 and iron-doped ZrO_2 samples.

The results obtained from electrochemical studying of these samples indicated that iron enhances the electrocatalytic properties of ZrO_2 towards the oxidation of TCP. However, doping of 1 % pushed the reaction toward the formation

of quinons, while the higher iron content directed the reaction also towards the formation of polymer film and the passivation of electrode.

TABLE III. The electrochemical parameters extracted from the EIS data in 1 mM TCP + 0.1 M H_2SO_4 (R_s – the solution resistance; R_{ct} – the charge transfer resistance; Y – CPE admittance, n – CPE exponent)

Sample	At potential of 0.80 V			At potential of 0.93 V					At potential of 1.10 V		
	R_{ct} / kΩ	Y / μS s^n	n	R_{ct} / kΩ	Y_1 / μS s^n	n	Y_2 / μS s^n	n	R_{ct} / MΩ	Y / μS s^n	n
ZrO_2	229	5.6	0.9	11.0	23.9	0.6	4.4	0.9	1.0	4.4	0.8
1-ZrO_2	267	4.9	0.8	9.9	20.7	0.6	4.1	0.8	1.8	3.8	0.8
5-ZrO_2	314	4.3	0.8	7.6	27.6	0.5	3.1	0.8	2.1	3.2	0.8
10-ZrO_2	369	4.0	0.8	7.0	28.7	0.5	2.5	0.8	2.5	3.1	0.8
20-ZrO_2	295	3.7	0.8	5.2	31.4	0.4	2.1	0.8	3.1	3.0	0.8

CONCLUSION

Solvothermaly synthesized pure and Fe-doped zirconia nanopowders were applied on the surface of glassy carbon electrode by Nafion and tested in the reaction of electrooxidation of 2,4,6-trichlorophenol (TCP). Cyclic voltam-mograms of all investigated electrodes showed the characteristic peak of oxidation of hydroxyl group at TCP and the reversible pair of peaks ascribed to the formation of quinones. Investigation of the electrodes based on pure and doped zirconium oxide nanopowders revealed that the amount of iron present in the sample influenced the pathway of TCP oxidation. The increase of iron content led to the increase of the current of TCP electrooxidation. However, the different iron content led to the various pathways of TCP electrooxidation. The low iron doping (1-ZrO_2) favoured the formation of quinons, while the samples with iron ion content higher than 1 % favoured the formation of polyphenol film on the electrode surface and the passivation of electrode. The 5-ZrO_2 electrode showed mixed behaviour reflected in the slight degradation of polyphenol film formed on this electrode.

Acknowledgement. This work was supported by the Ministry for Education, Science and Technological Development of the Republic of Serbia (Grants No. 451-03-68/2020-14/ /200026 and 451-03-68/2020-14/200017).

И З В О Д

ЕЛЕКТРОХЕМИЈСКА ОКСИДАЦИЈА 2,4,6-ТРИХЛОРФЕНОЛА НА НАНО-ЦИРКОНИЈУМ-ОКСИДНОЈ МАРТИЦИ ДОПИРАНОЈ ГВОЖЂЕМ

НАДИЦА Д. АБАЗОВИЋ[1], ТАТЈАНА Д. САВИЋ[1], ТАТЈАНА Б. НОВАКОВИЋ[2], МИРЈАНА И. ЧОМОР[1] и ЗОРИЦА Д. МОЈОВИЋ[2]

[1]Институт за нуклеарне науке Винча – Институт од националног значаја за Републику Србију – Универзитет у Београду, Београд и [2]Универзитет у Београду – Институт за хемију, технологију и металургију – Институт од националног значаја за Републику Србију, Његошева 12, 11000 Београд

Нанопрахови цирконијум-оксида, чисти и допирани различитим количинама јона гвожђа синтетисани су солвотермалном методом. Добијени прахови су коришћени као

модификатори електрода од стакластог угљеника. Модификоване електроде су тестиране у реакцији електрохемијске оксидације 2,4,6-трихлорфенола (TCP), како би се испитао утицај допанта на перформансе цирконијум-оксидне матрице. За испитивање су коришћене технике цикличне волтаметрије и електрохемијске импедансне спектроскопије. Резултати цикличне волтаметрије су показали да се електрооксидација TCP одиграва преко оксидације хидроксилне групе. Могуће даље реакционе путање су укључивале формирање хинона и настајање полифенолног филма на површини електроде који доводи до пасивације електроде. Допирање јонима гвожђа је повећало активност цирконијум-оксидне матрице за електрооксидацију TCP. Резултати електрохемијске импедансне спектроскопије су указали на утицај количине јона гвожђа у цирконијум-оксидној матрици на реакциони механизам TCP електроосидације. Реакциона путања која укључује формирање хинона је фаворизована на цирконијум-оксидним електродама са ниским садржајем јона гвожђа (допираног са 1 % јона гвожђа), док је формирање полифенолног филма дошло до изражаја на узорцима са већим садржајем јона гвожђа (допираних са 10 и 20 % јона гвожђа). Узорак цирконијум-оксида, допиран са 5 % јона гвожђа, има прелазна својства, јер долази до формирања полифенолног филма на површини електроде, али и до његове разградње.

(Примљено 4. августа, ревидирано 13. новембра, прихваћено 30. новембра 2020)

REFERENCES

1. C. Terashima, T. N. Rao, D. A. Tryk, A. Fujishima, *Anal. Chem.* **74** (2002) 895 (https://doi.org/10.1021/ac010681w)
2. M. Saraji, M. Ghani, *J. Chromatogr., A* **1418** (2015) 45 (https://doi.org/10.1016/j.chroma.2015.09.062)
3. S. Almeda, L. Nozal, L. Arce, M. Valcárcel, *Anal. Chim. Acta* **587** (2007) 97 (https://doi.org/10.1016/j.aca.2007.01.035)
4. Y. Higashi, Y. Fujii, *J. Liq. Chromatogr. Relat. Technol.* **32** (2009) 2372 (https://doi.org/10.1080/10826070903188013)
5. A. J. Barik, P. R. Gogate, *Ultrason. Sonochem.* **40** (2018) 383 (https://doi.org/10.1016/j.ultsonch.2017.07.029)
6. C. Tai, G. Jiang, *Chemosphere* **59** (2005) 321 (https://doi.org/10.1016/j.chemosphere.2004.10.024)
7. J. Xiong, C. Hang, J. Gao, Y. Guo, C. Gu, *Chem. Eng. J.* **254** (2014) 276 (https://doi.org/10.1016/j.cej.2014.05.139)
8. L. Wang, D. Kong, Y. Ji, J. Lu, X. Yin, Q. Zhou, *Chem. Eng. J.* **343** (2018) 235 (https://doi.org/10.1016/j.cej.2018.03.006)
9. M. Shabani-Nooshabadi M, Roostaee, F. Tahernejad-Javazmi, *J. Mol. Liq.* **219** (2016) 142 (https://doi.org/10.1016/j.molliq.2016.01.081)
10. S. Hashemnia, Sh. Khayatzadeh, M. Hashemnia, *J. Solid State Electrochem.* **16** (2012) 473 (https://doi.org/10.1007/s10008-011-1355-2)
11. C. Comninellis, A. Nerini, *J. Appl. Electrochem.* **25** (1995) 23 (https://doi.org/10.1007/BF00251260)
12. Z. Sun, X. Ma, X. Hu, *Environ. Sci. Pollut. Res*. **24** (2017) 14355 (https://doi.org/10.1007/s11356-017-9004-7)
13. Y. Yao, L. Jiao, N. Yu, J. Zhu, X. Chen, *Russ. J. Electrochem.* **52** (2016) 348 (https://doi.org/10.1134/S1023193516040157)
14. M. S. Ureta-Zañartu, P. Bustos, M. C. Diez, M. L. Mora, C. Gutiérrez, *Electrochim. Acta* **46** (2001) 2545 (https://doi.org/10.1016/S0013-4686(01)00448-0)

15. F. Fernández, C. Berríos, E. Garrido-Ramírez, N. Escalona, C. Gutiérrez, M. S. Ureta-Zañartu, *J. Appl. Electrochem.* **44** (2014) 1295 (https://doi.org/10.1007/s10800-014-0763-2)
16. C. Berríos, J. F. Marco, C. Gutiérrez, M. S. Ureta-Zañartu, *Electrochim. Acta* **54** (2009) 6417 (https://doi.org/10.1016/j.electacta.2009.06.017)
17. C. Berríos, R. Arce, M. C. Rezende, M. S. Ureta-Zañartu, C. Gutiérrez, *Electrochim. Acta* **53** (2008) 2768 (https://doi.org/10.1016/j.electacta.2007.10.053)
18. M. S. Ureta-Zañartu, M. L. Mora, M. C. Diez, C. Berríos, J. Ojeda, C. Gutiérrez, *J. Appl. Electrochem.* **32** (2002) 1211 (https://doi.org/10.1023/A:1021680420834)
19. M. S. Ureta-Zañartu, C. Berríos, J. Pavez, J. Zagal, C. Gutiérrez, J. F. Marco, *J. Electroanal. Chem.* **553** (2003)147 (https://doi.org/10.1016/S0022-0728(03)00309-7)
20. M. S. Ureta-Zañartu, P. Bustos, C. Berríos, M. C. Diez, M. L. Mora, C. Gutiérrez, *Electrochim. Acta* **47** (2002) 2399 (https://doi.org/10.1016/S0013-4686(02)00043-9)
21. W. Xia, F. Wang, X. Mu, K. Chen, *React. Kin. Mech. Catal.* **122** (2017) 463 (https://doi.org/10.1007/s11144-017-1193-z)
22. Y. Wang, X. Yang, Y. Chen, S. Nie, M. Xie, *React. Kin. Mech. Catal.* **122** (2017) 915 (https://doi.org/10.1007/s11144-017-1243-6)
23. M. V. Carević, N. D. Abazović, T. D. Savić, T. B. Novaković, D. J. Pjević, M. I. Čomor, *J. Am. Ceram. Soc.* **101** (2018) 1420 (https://doi.org/10.1111/jace.15324)
24. K. C. Soni, S. C. Shekar, B. Singh, T. Gopi, *J. Colloid Interface Sci.* **446** (2015) 226 (https://doi.org/10.1016/j.jcis.2015.01.031)
25. M. V. Carević, T. D. Savić, N. D. Abazović, M. D. Mojović, T. B. Novaković, M. I. Čomor, *Ceram. Int.* **46** (2020) 6820 (https://doi.org/10.1016/j.ceramint.2019.11.175)
26. A. Doménech-Carbó, G. Herrera, N. Montoya, P. Pardo, J. Alarcón, M. T. Doménech-Carbó, M. Silva, *J. Electrochem. Soc.* **161** (2014) H539 (https://doi.org/10.1149/2.0751409jes)
27. G. Herrera, N. Montoya, A. Domenech, J. Alarcón, *Phys. Chem. Chem. Phys.* **15** (2013) 19312 (https://doi.org/10.1039/C3CP53216J)
28. A. Doménech-Carbó, M. T. Doménech-Carbó, J. V. Gimeno-Adelantado, F. Bosch-Reig, M. C. Saurí-Peris, S. Sánchez-Ramosa, *Analyst* **126** (2001) 1764 (https://doi.org/10.1039/B100257K)
29. K. W. Cho, V. S. Rao, H.S. Kwon, *Electrochim. Acta* **52** (2007) 4449 (https://doi.org/10.1016/j.electacta.2006.12.032)
30. H. Al-Maznai, B. E. Conway, , *J. Serb. Chem. Soc.* **66** (2001) 765 (https://doi.org/10.2298/JSC0112765A)
31. Z. Ežerskis, Z. Jusys, *J. Appl. Electrochem.* **31** (2001) 1117 (https://doi.org/10.1023/A:1012280216273).